Pergamon

Int. J. Solids Structures Vol. 35, No. 14, pp. 1575–1587, 1998

0020–7683/98 $19.00 + .00

PII: S0020–7683(97)00127–3

AN ANALYTICAL SOLUTION FOR CROSS-PLY LAMINATES UNDER CYLINDRICAL BENDING BASED ON THROUGH-THE-THICKNESS INEXTENSIBILITY. PART II—VIBRATIONS

S. JAVAD JALALI and FARID TAHERI
Department of Civil Engineering, Technical University of Nova Scotia P.O. Box 1000, Halifax, Nova Scotia, Canada B3J 2X4

(*Received* 2 *June* 1996; *in revised form* 6 *May* 1997)

Abstract—The dynamic behavior of cross-ply laminated plates under cylindrical and/or planar bending is considered. The methodology introduced in Part I is extended for treating the transverse vibration of laminated plates. The solution for a simply-supported plate at two ends is obtained. Natural frequencies and the corresponding stress distribution for several cases are presented. Also, we employed a new procedure for finding the exact natural frequencies and the corresponding stresses based on the elasticity solution presented by Jones (1970). The proposed procedure significantly increases the capability of the elasticity solution and eliminates most of the problems experienced by the previous researchers in the application of the solution for higher modes and multi-layer laminates. The comparison of the results obtained by the introduced method and the elasticity solution validates the integrity of the introduced method. The results are also obtained by finite element method and one of the higher-order laminated plate theories. The investigation shows the inadequacy of the higher-order theory in predicting the stresses. Also the results obtained by finite element method show that by increasing the mode number of vibration, to obtain a satisfactory result, a finer mesh is necessary. Furthermore, the shear stresses at the interface at two adjacent layers are more likely to be inaccurate. © 1998 Elsevier Science Ltd.

FORMULATION

Following up of the work done in Part I (Jalali and Taheri, 1998), we apply the assumption of the through-the-thickness inextensibility to the transverse vibration of cross-ply laminated plates. A short review of the literature has been given in part I of this work, therefore, here we only proceed with the application of the introduced method. In the previous work we used the engineering strain, γ_{xz} and γ_{yz}, for developing a displacement field through the thickness of the plate. We showed that:

$$u = -z\frac{\partial w}{\partial x} + u^0 + \int_0^z \gamma_{xz}\,\mathrm{d}z \tag{1a}$$

$$v = -z\frac{\partial w}{\partial y} + v^0 + \int_0^z \gamma_{yz}\,\mathrm{d}z, \tag{1b}$$

where u and v are the in-plane displacements in the x- and y-direction, respectively, and w denotes the out-of-plane displacement in the z-direction. Also, u^0 and v^0 refer to the corresponding in-plane displacement at $z = 0$. The Cartesian coordinate system is adopted and; as shown in Fig. 1, is constructed on the center line of the laminate at $x = 0$. Also, a local coordinate is defined on the center line of each layer. Since we are only concerned with the variables in the x-direction, for simplicity, we omit the subscripts. Therefore, σ and ε are the stress and strain in the x-direction and τ is the through-the-thickness shear stress in zy plane, respectively. The laminate is simply-supported at two ends. Therefore, the boundary conditions at two ends are defined as:

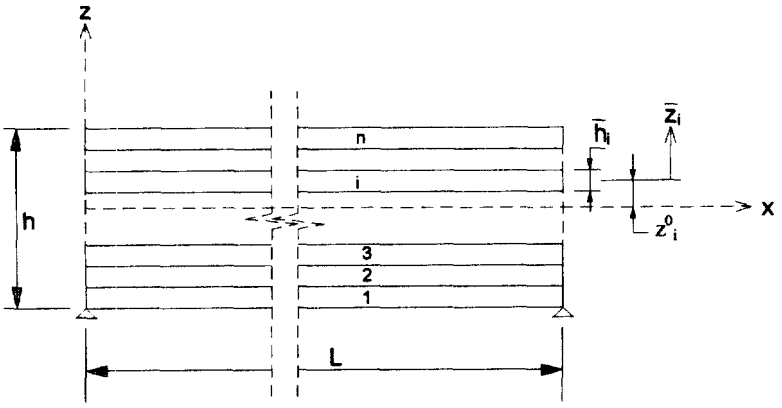

Fig. 1. The coordinate systems of laminates.

$$x = 0, L \begin{cases} w = 0 \\ \sigma_i = 0, \quad i = 1, 2, \ldots, n, \end{cases} \tag{2}$$

where subscript i indicates the layer number and n is the total number of layers. The constitutive relationship within each layer for the cylindrical and planar bending can be simplified in the following identical form:

$$\sigma = \bar{E}\varepsilon$$
$$\tau = G\gamma, \tag{3}$$

where G and $\bar{E}$ are the corresponding shear modulus in zy plane and the longitudinal stiffness in the x-direction, respectively. In the case of beam type problem (planar bending) the longitudinal stiffness is equal to the modulus of elasticity in the x-direction. However, for cylindrical bending it is equal to:

$$\bar{E} = \frac{E_{11}}{1 - \upsilon_{12}\upsilon_{21}}, \tag{4}$$

where E and υ are the elastic modulus and the Poisson's ratio of the layer and subscripts 1 and 2 refer to the x- and y-direction, respectively.

The first derivative of eqn (1a) with respect to x gives the longitudinal strain, ε. Multiplying the result by longitudinal stiffness, we can find the longitudinal stress of each layer as

$$\sigma_i = -\bar{z}_i\bar{E}_i\frac{\mathrm{d}^2 w}{\mathrm{d}x^2} + \bar{E}_i\frac{\mathrm{d}u_i^0}{\mathrm{d}x} + \frac{\bar{E}_i}{G_i}\int_0^{z_i}\frac{\mathrm{d}\tau_i}{\mathrm{d}x}\mathrm{d}\bar{z}_i. \tag{5}$$

The equilibrium condition in the x-direction is:

$$\frac{\partial\sigma_i}{\partial x} + \frac{\partial\tau_i}{\partial\bar{z}_i} = \rho_i\frac{\partial^2 u_i}{\partial t^2}, \tag{6}$$

where ρ is the mass density of the layer. Substituting eqns (1a), (3) and (5) in eqn (6) gives

$$\frac{\partial\tau_i}{\partial\bar{z}_i} = \bar{z}_i\bar{E}_i\frac{\partial^3 w}{\partial x^3} - \bar{E}_i\frac{\partial^2 u_i^0}{\partial x^2} - \frac{\bar{E}_i}{G_i}\int_0^{z_i}\frac{\partial^2\tau_i}{\partial x^2}\mathrm{d}\bar{z}_i + \rho_i\left(-\bar{z}_i\frac{\partial^3 w}{\partial x\,\partial t^2} + \frac{\partial^2 u_i^0}{\partial t^2} + \frac{1}{G_i}\int_0^{z_i}\frac{\partial^2\tau_i}{\partial t^2}\mathrm{d}\bar{z}_i\right). \tag{7}$$

The differential equation (7), in case of free vibration, has two types of solutions. The

solution depend on the value of w. For $w = 0$, eqn (7) leads to two different kinds of longitudinal type vibrations. However, for $w \neq 0$, we will reach the solution of transversal vibration. In this paper, we will concentrate on addressing the problem of transversal vibration. In this case the solution of eqn (7) has the following form:

$$w = w_0 \sin(px) \sin(\omega t) \tag{8a}$$

$$q = q_0 \sin(px) \sin(\omega t) \tag{8b}$$

$$\tau_i = B_i \cos(px) \sin(\omega t) \tag{8c}$$

$$u_i^0 = c_i \cos(px) \sin(\omega t), \tag{8d}$$

where

$$p = \frac{m\pi}{L},$$

and m and ω denote the vibration mode number and the corresponding frequency, respectively. B_i is a function of $\bar{z}_i$, but w_0 and c_i are constants. Substituting eqn (8) in eqn (7) leads to:

$$\frac{dB}{d\bar{z}_i} = -\bar{z}_i \bar{E}_i w_0 p^3 \left(1 - \frac{\rho_i \omega^2}{\bar{E}_i p^2}\right) + c_i \bar{E}_i p^2 \left(1 - \frac{\rho_i \omega^2}{\bar{E}_i p^2}\right) + \frac{\bar{E}_i}{G_i} p^2 \left(1 - \frac{\rho_i \omega^2}{\bar{E}_i p^2}\right) \int_0^{\bar{z}_i} B_i \, d\bar{z}_i. \tag{9}$$

Equations (8) satisfy the boundary conditions for the simply-supported plate at its two ends.

Recognizing eqn (8c) the boundary conditions on the bottom and top of each layer are defined as:

$$\begin{aligned} \tau_i^B &= \tau_i^- \cos(px) \sin(\omega t) \\ \tau_i^T &= \tau_i^+ \cos(px) \sin(\omega t), \end{aligned} \tag{10a}$$

or

$$\begin{aligned} B_i(-\bar{h}_i/2) &= \tau_i^- \\ B_i(+\bar{h}_i/2) &= \tau_i^+. \end{aligned} \tag{10b}$$

Using the Laplace transformation and applying the boundary conditions at $\bar{z}_i = \pm \bar{h}_i/2$, we can find the solution of the above differential equation. That is:

$$B_i = \left(\frac{\tau_i^+ + \tau_i^-}{2}\right) \frac{\cosh(\sqrt{\beta_i}\bar{z}_i)}{\cosh(\sqrt{\beta_i}\bar{h}_i/2)} + \left(\frac{\tau_i^+ - \tau_i^-}{2}\right) \frac{\sinh(\sqrt{\beta_i}\bar{z}_i)}{\sinh(\sqrt{\beta_i}\bar{h}_i/2)} + w_0 G_i p \left[1 - \frac{\cosh(\sqrt{\beta_i}\bar{z}_i)}{\cosh(\sqrt{\beta_i}\bar{h}_i/2)}\right], \tag{11a}$$

$$c_i = \frac{\tau_i^+ - \tau_i^-}{2\bar{E}_i} \frac{\sqrt{\beta_i}}{\sinh(\sqrt{\beta_i}\bar{h}_i/2)}, \tag{11b}$$

where

$$\beta_i = \frac{\bar{E}_i p^2}{G_i}\left(1 - \frac{\rho_i \omega^2}{\bar{E}_i p^2}\right). \tag{12}$$

Substituting eqns (11) and (8) in eqn (5), one can obtain the relation for longitudinal stress.

$$\sigma_i = p\bar{E}_i \begin{bmatrix} \dfrac{w_0 p}{\sqrt{\beta_i}} \dfrac{\sinh(\sqrt{\beta_i}\bar{z}_i)}{\cosh(\sqrt{\beta_i}\bar{h}_i/2)} - \left(\dfrac{\tau_i^+ + \tau_i^-}{2G_i\sqrt{\beta_i}}\right) \dfrac{\sinh(\sqrt{\beta_i}\bar{z}_i)}{\cosh(\sqrt{\beta_i}\bar{h}_i/2)} \\ -\left(\dfrac{\tau_i^+ - \tau_i^-}{2G_i\sqrt{\beta_i}}\right) \dfrac{\cosh(\sqrt{\beta_i}\bar{z}_i)}{\sinh(\sqrt{\beta_i}\bar{h}_i/2)} \end{bmatrix} \sin(px)\sin(\omega t). \tag{13}$$

Substituting eqn (11a) in eqn (8c) and integrating over the thickness gives the corresponding shear force of each layer. The shear force at any section of the laminate is equal to the sum of the shear forces of individual layers. Moreover, the sectional shear force is related to the inertia force by the following relations:

$$\frac{\mathrm{d}V}{\mathrm{d}x} = -q, \tag{14a}$$

and

$$q = -\bar{m}\frac{\partial^2 w}{\partial t^2}, \tag{14b}$$

in which V and $\bar{m}$ are the shear force at the section and the distributed mass of the plate, respectively. The above statements can be written in the mathematical form by

$$\sum_{i=1}^{n} \frac{\tau_i^+ + \tau_i^-}{\sqrt{\beta_i}} \tanh(\sqrt{\beta_i}\bar{h}_i/2) + w_0 p \sum_{i=1}^{n} G_i \left[\bar{h}_i - \frac{2}{\sqrt{\beta_i}} \tanh(\sqrt{\beta_i}\bar{h}_i/2)\right] = \frac{w_0 \bar{m}\omega^2}{p}. \tag{15}$$

The longitudinal displacement of each layer is found by substituting eqns (11) and (8) in eqn (1a) as:

$$u_i = \begin{bmatrix} \dfrac{\tau_i^+ + \tau_i^-}{2G_i\sqrt{\beta_i}} \dfrac{\sinh(\sqrt{\beta_i}\bar{z}_i)}{\cosh(\sqrt{\beta_i}\bar{h}_i/2)} + \dfrac{\tau_i^+ - \tau_i^-}{2G_i\sqrt{\beta_i}} \dfrac{\cosh(\sqrt{\beta_i}\bar{z}_i)}{\sinh(\sqrt{\beta_i}\bar{h}_i/2)} \\ -\dfrac{w_0 p}{\sqrt{\beta_i}} \dfrac{\sinh(\sqrt{\beta_i}\bar{z}_i)}{\cosh(\sqrt{\beta_i}\bar{h}_i/2)} \end{bmatrix} \cos(px)\sin(\omega t). \tag{16}$$

For oscillatory type problems, stresses and displacements at any point are proportional to the amplitude of vibration. Taking w_0 as the amplitude of vibration, all the other variables can be written as a ratio of w_0. Since the frequency is independent of the amplitude of vibration, we can arbitrarily take $w_0 = 1$. For a laminate consisting of n layers, there are $n-1$ unknown shear stresses at the interface of adjacent layers and also one unknown frequency. Enforcing the compatibility condition at the interface of adjacent layers by equating the corresponding longitudinal displacements from eqn (16), gives $n-1$ equations. These equations along with eqn (15), will produce a sufficient number of equations to solve for the n unknowns. However, one should remember that the elements of the coefficient matrix are a function of frequency and, therefore, the solution of the simultaneous equations needs some extra consideration. The last term in eqn (12) represents the effect of rotary inertia. The value of this term comparing to unity is always small and has little effect on the solution. However, a fast convergence can be obtained when an iteration method based on updating ω in eqn (12) is adopted. For the first iteration the effect of rotary inertia can

be neglected. Two or three iterations will be sufficient for convergency. As it will be shown later, the final result is very close to the result of the first iteration, and for the practical purposes there is no need to include the effect of rotary inertia. Knowing the interfaces' shear stresses and the frequency of vibration, the calculation of stresses are straightforward by using eqns (11a) and (13).

For unidirectional laminates consisting of only one type of layer the solution is simplified as follows:

$$\omega^2 = \frac{p^2 G}{\rho}\left[1 - \frac{\tanh(\sqrt{\beta}h/2)}{\sqrt{\beta}h/2}\right], \tag{17}$$

$$\sigma = w_0 \frac{p^2 \bar{E}}{\sqrt{\beta}} \times \frac{\sinh(\sqrt{\beta}z)}{\cosh(\sqrt{\beta}h/2)} \sin(px)\sin(\omega t), \tag{18}$$

$$\tau = w_0 Gp\left[1 - \frac{\cosh(\sqrt{\beta}z)}{\cosh(\sqrt{\beta}h/2)}\right]\cos(px)\sin(\omega t). \tag{19}$$

Exact solution

The exact elasticity solution for cross-ply laminate was given by Jones (1970). He had the problem of the complexity of the procedure when the number of layers became moderately large and, therefore, his work was limited to two-layer plates. Kulkarni and Pagano (1972) had the same problem for angle-ply laminates and their work was limited to five-layer plates. Furthermore, the accuracy of both solutions diminished as larger mh/L ratios were considered and, therefore, they limited their work to $mh/L < 1$ and $mh/L < 1.2$, respectively. In order to be able to verify the integrity of the method presented in this paper it was necessary to have the results of the exact solution for much wider range. For this, we have employed a new procedure for finding the exact natural frequency and the stress distribution of the laminates. The procedure is based on the solution given by Jones (1970) and is discussed below.

The displacement functions of each layer in the x- and z-directions can be written in the following form:

$$u_i = \left[\sum_{j=1}^{4} A_j \left(\frac{d\lambda_i^2 + e}{c\lambda_j}\right)\exp(\lambda_j \bar{z}_i)\right]\cos(px)\sin(\omega t), \tag{20a}$$

$$w_i = \left[\sum_{j=1}^{4} A_j \exp(\lambda_j \bar{z}_i)\right]\sin(px)\sin(\omega t), \tag{20b}$$

where

$$\lambda = \pm\sqrt{\frac{-c^2 - ae - bd \pm \sqrt{(c^2 + ae + bd)^2 - 4bead}}{2ad}}, \tag{21}$$

and

$$a = R_{66} = G_{xz}, \quad b = \rho\omega^2 - p^2 R_{11},$$
$$c = p(R_{13} + R_{66}), \quad d = R_{33},$$
$$e = \rho\omega^2 - p^2 R_{66}.$$

R_{11}, R_{33} and R_{13} are the stiffness coefficients of material in plane strain condition where subscripts 1 and 3 denote the x- and z-direction, respectively. There are four unknowns (as denoted by A_j) for each layer in the above equations. The stresses are:

$$(\sigma_x)_i = \left\{\sum_{j=1}^{4} A_j\left[-R_{11}p\frac{d\lambda_j^2+e}{c\lambda_j}+R_{13}\lambda_j\right]\exp(\lambda_j\bar{z}_i)\right\}\sin(px)\sin(\omega t), \tag{22a}$$

$$(\sigma_z)_i = \left\{\sum_{j=1}^{4} A_j\left[-R_{13}p\frac{d\lambda_j^2+e}{c\lambda_j}+R_{33}\lambda_j\right]\exp(\lambda_j\bar{z}_i)\right\}\sin(px)\sin(\omega t), \tag{22b}$$

$$(\tau_{xz})_i = \left\{\sum_{j=1}^{4} A_j R_{66}\left[\frac{d\lambda_j^2+e}{c}+p\right]\exp(\lambda_j\bar{z}_i)\right\}\cos(px)\sin(\omega t). \tag{22c}$$

Equations (20) and (22) satisfy the boundary conditions at two ends of the plate, as expressed by eqn (2). There are also eight other boundary conditions for each layer, which are u, w, σ_y and τ_{xz} at the top and bottom of each layer. Equating these boundary values of each layer to the corresponding values of the adjacent layers gives $4n$ linear equations in which the values of A are unknown. In the absence of any external load, the right-hand side of all the equations is zero. Therefore, to obtain a nontrivial solution for this set of simultaneous equations, it is necessary that the determinant of the coefficient matrix to be equal to zero. The elements of the coefficient matrix are a function of ω^2 and for a certain values of ω^2 the determinant of the matrix will become zero. However, since the relations between the elements of coefficient matrix and ω^2 are in trigonomeric and hyperbolic forms, the usual methods for the eigenvalue problems cannot be used in here.

To obtain the values of ω, we employ a trial and error procedure. The procedure requires an initial value for ω, and calculates the determinant of the coefficient matrix. To make the determinant equal to zero, at each iteration the value of ω is corrected until the values of ω from two iterations are quite close. It has been observed that the success of the procedure is strongly dependent on the initial value of ω. The procedure will converge to the exact value of ω, as long as the initial value is not too far from its exact value. For this purpose, the ω values obtained from the method developed earlier in this paper have enough accuracy, and can be used as the initial values for the procedure.

Higher-order laminated plate theory

The higher-order laminated plate theory (HLPT) presented by Reddy (1989) is considered in this part. To keep the formulation as simple as possible, in this part we only discuss the symmetric laminate. Readers should note, however, that there is no limitation for the application of either of the methods (i.e. the method presented in this paper or HLPT), for unsymmetric laminates. The displacement field in HLPT is as follows:

$$u = u^0 + z\left[\varphi_x - \frac{4}{3}\left(\frac{z}{h}\right)^2\left(\varphi_x + \frac{\partial w}{\partial x}\right)\right], \tag{23a}$$

$$v = v^0 + z\left[\varphi_y - \frac{4}{3}\left(\frac{z}{h}\right)^2\left(\varphi_y + \frac{\partial w}{\partial y}\right)\right]. \tag{23b}$$

These equations can easily be found by assuming a parabolic distribution of shear strain through the thickness of plate and substituting in eqn (1). For cylindrical and/or planar bending the constitutive relationship and the equilibrium equations are the same as eqns (3) and (6), respectively. The solution of the problem with boundary conditions expressed by eqn (2) is in the following form.

$$w = w_0 \sin(px)\sin(\omega t)$$
$$\varphi_x = \varphi_0 \cos(px)\sin(\omega t). \tag{24}$$

Substituting these equations in eqn (23a) and recalling eqn (14), one obtains the following equation for symmetric laminates:

$$\left[\frac{1}{p}\left(I_1-\frac{4I_2}{3h^2}\right)\frac{I_0}{A_{55}-\dfrac{4D_{55}}{h^2}}\right]\omega^4-\left[\left(D_{11}-\frac{4F_{11}}{3h^2}\right)\frac{pI_0}{A_{55}-\dfrac{4D_{55}}{h^2}}+\frac{I_0}{p}+pI_1\right]\omega^2+p^3D_{11}=0, \tag{25}$$

where

$$D_{11}=\int_{-h/2}^{h/2}\bar{E}z^2\,\mathrm{d}z,\quad F_{11}=\int_{-h/2}^{h/2}\bar{E}z^4\,\mathrm{d}z,$$

$$A_{55}=\int_{-h/2}^{h/2}G\,\mathrm{d}z,\quad D_{55}=\int_{-h/2}^{h/2}Gz^4\,\mathrm{d}z,$$

$$I_0=\bar{m}=\int_{-h/2}^{h/2}\rho\,\mathrm{d}z,\quad I_1=\int_{-h/2}^{h/2}\rho z^2\,\mathrm{d}z,\quad I_2=\int_{-h/2}^{h/2}\rho z^4\,\mathrm{d}z.$$

The natural frequency of the plate, hence can be found from eqn (25). The axial stress in the x-direction is obtained directly by multiplication of the axial stiffness by the first derivative of u with respect to x. That is:

$$\sigma_i=z\bar{E}_i\left[-p\varphi_0+\frac{4}{3}\left(\frac{z}{h}\right)^2(p\varphi_0+p^2)\right], \tag{26}$$

where

$$\varphi_0=w_0\left(\frac{\omega^2I_0}{p\left(A_{55}-\dfrac{4}{h^2}D_{55}\right)}-p\right). \tag{27}$$

However, the through-the-thickness shear stress is obtained by substituting eqn (26) in equilibrium equation (6). This procedure leads to the following equation for the shear stresses of two different points in the same layer:

$$\tau_2^i-\tau_1^i=\left[\frac{\varphi_0}{2}(z_2^2-z_1^2)-\frac{1}{3h^2}(z_2^4-z_1^4)(p+\varphi_0)\right](p^2\bar{E}_i-\rho_i\omega^2). \tag{28}$$

To calculate the shear stresses, it is necessary to start from the outer most layers, where the shear stress at top or bottom of the layer is zero, and proceed to the adjacent layers.

NUMERICAL RESULTS

In this part we verify the integrity of the proposed method. Natural frequency and the modal stresses of different laminates are obtained and the results are compared with the results obtained by the exact elasticity solution (Jones, 1970), the higher-order laminated plate theory (HLPT) of Reddy (1989) and the finite element method (FEM) (NISA II, 1995). Four configurations of layup, as described below are considered:

(Case 1) unidirectional laminate with the fibers oriented in the x-direction (0° laminate);
(Case 2) laminate composed of five layers with equal thickness [0/90/0/90/0];
(Case 3) laminate composed of 10 layers with equal thickness $[(0/90/0/90/0)_S]$;
(Case 4) laminate composed of 20 layers with equal thickness $[(0/90)_5]_S$.

In all cases, we assume that the laminate has total thickness of 2 mm and the span length is 20 mm. Also, we assume the properties of the layers are as follows:

$$E_L = 174.6\ \text{GPa}, \quad E_T = 7\ \text{GPa},$$
$$G_{LT} = 3.5\ \text{GPa}, \quad G_{TT} = 1.4\ \text{GPa},$$
$$v_{LT} = v_{TT} = 0.25, \quad \rho = 1700\ \text{kg m}^{-3}, \tag{29}$$

where L and T are the directions parallel and normal to the fibers, respectively.

The finite element methods were constructed by using quadratic 8-noded plane strain elements. Half of the beam was considered and, therefore, the results could not carry the transverse vibration with even mode numbers. Accuracy and the convergent of FEM analysis were examined by considering four different mesh schemes. The specifications of the mesh schemes are tabulated in Table 1.

The natural frequencies of the laminates for the first 50 mode shapes were obtained by using the above-mentioned different methods. Part of the results for laminate cases 1 and 4 are presented in Tables 2 and 3, respectively. The results show a very good agreement between the results of the present method and those of the exact values. The convergence of the results obtained by the FEM to the exact values also confirms the procedure used in conjunction with the exact solution (Jones, 1970) for obtaining the exact frequencies. The

Table 1. The specification of FEM mesh schemes

Mesh scheme designation	No. of elements in depth	No. of elements in half span	Element size mm
FEM1	4	20	0.5×0.5
FEM2	10	50	0.2×0.2
FEM3	20	100	0.1×0.1
FEM4	30	150	0.06667×0.06667

Table 2. Frequencies (rad s^{-1}) obtained by different methods for case I

Mode no.	Present method with rotary inertia effect	Present method without rotary inertia effect	Elasticity	FEM2	FEM4	HLPT
1	1.1817×10^5	1.1839×10^5	1.1820×10^5	1.1820×10^5	1.1820×10^5	1.18×10^5
5	1.0195×10^6	1.0205×10^6	1.0192×10^6	1.0192×10^6	1.0192×10^6	9.89×10^5
9	1.9234×10^6	1.9244×10^6	1.9218×10^6	1.9218×10^6	1.9218×10^6	1.83×10^6
15	3.2768×10^6	3.2778×10^6	3.2731×10^6	3.2731×10^6	3.2731×10^6	3.07×10^6
21	4.6296×10^6	4.6306×10^6	4.6235×10^6	4.6242×10^6	4.6235×10^6	4.31×10^6
27	5.9821×10^6	5.9832×10^6	5.9737×10^6	5.9761×10^6	5.9737×10^6	5.55×10^6

Table 3. Frequencies (rad s^{-1}) obtained by different methods for case 4

Mode no.	Present method with rotary inertia effect	Present method without rotary inertia effect	Elasticity	FEM3	HLPT
1	9.03695×10^4	9.05305×10^4	9.03906×10^4	9.0391×10^4	9.31×10^4
5	7.74073×10^5	7.74638×10^5	7.74105×10^5	7.7412×10^5	8.17×10^5
9	1.46280×10^6	1.46344×10^6	1.46264×10^6	1.4628×10^6	1.52×10^6
15	2.50962×10^6	2.51078×10^6	2.50925×10^6	2.5111×10^6	2.55×10^6
21	3.58073×10^6	3.58277×10^6	3.58043×10^6	3.5878×10^6	3.58×10^6
27	4.67324×10^6	4.67630×10^6	4.67312×10^6	4.6910×10^6	4.61×10^6

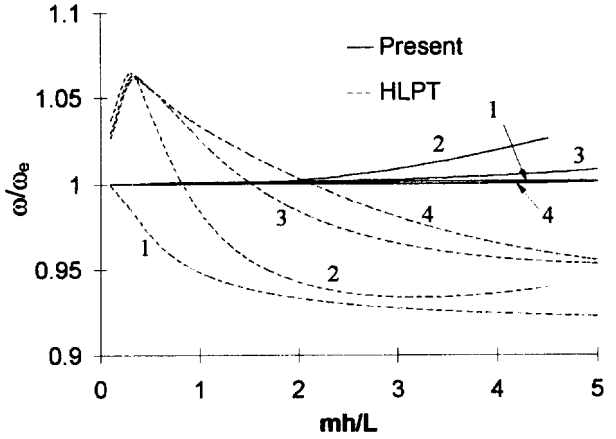

Fig. 2. The normalized frequencies with respect to the values of exact solution.

results of the HLPT are not as accurate as the other methods. In Fig. 2, the frequencies obtained by HLPT and the present method have been normalized to the exact values. For laminate case 2, the procedure developed to obtain the exact values, did not converge to the exact values for $mh/L > 4.5$ and, therefore, the corresponding curves were terminated at this point. As shown in this figure, for two more practical cases (cases 1 and 4), the results of the present method are practically identical to the exact values. However, the error from HLPT for all cases goes beyond 6%.

As previously explained, the elimination of the second term in eqn (12), which represents the effect of rotary inertia does not have a considerable effect on the results. This phenomenon can be seen from the values of columns 2 and 3 in Tables 2 and 3. Also, as shown in Fig. 3 the small difference between the frequencies obtained in two cases is quite negligible.

The distribution of shear and axial stresses through the thickness of the laminates for several modes was calculated by using the different methods. In all cases the amplitude of the vibration was taken as $w_0 = 1$ mm. In FEM and exact solution, however, because the deflection varies through the thickness, an average value of 1 mm was used. Figures 4–7 show the results of the calculations for three modes. As shown in these figures, the stresses obtained by the present method are in very close agreement to the exact values (in most cases they are practically identical). In general, the accuracy of the results decreases as the value of mh/L increases. It has been found that HLPT cannot produce accurate results even for the first mode ($mh/L = 0.1$). The discrepancy increases rapidly for higher modes and it becomes quite unacceptable after the third mode ($mh/L = 0.3$). This fact is shown in the figures illustrating the results for mode 5 (Figs 4–7).

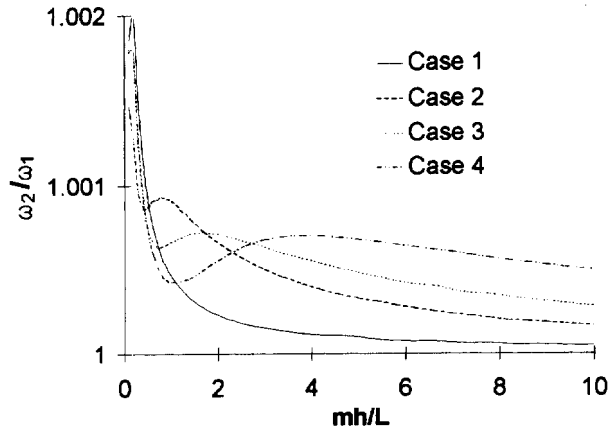

Fig. 3. The ratio of frequency obtained with and without considering rotary inertia.

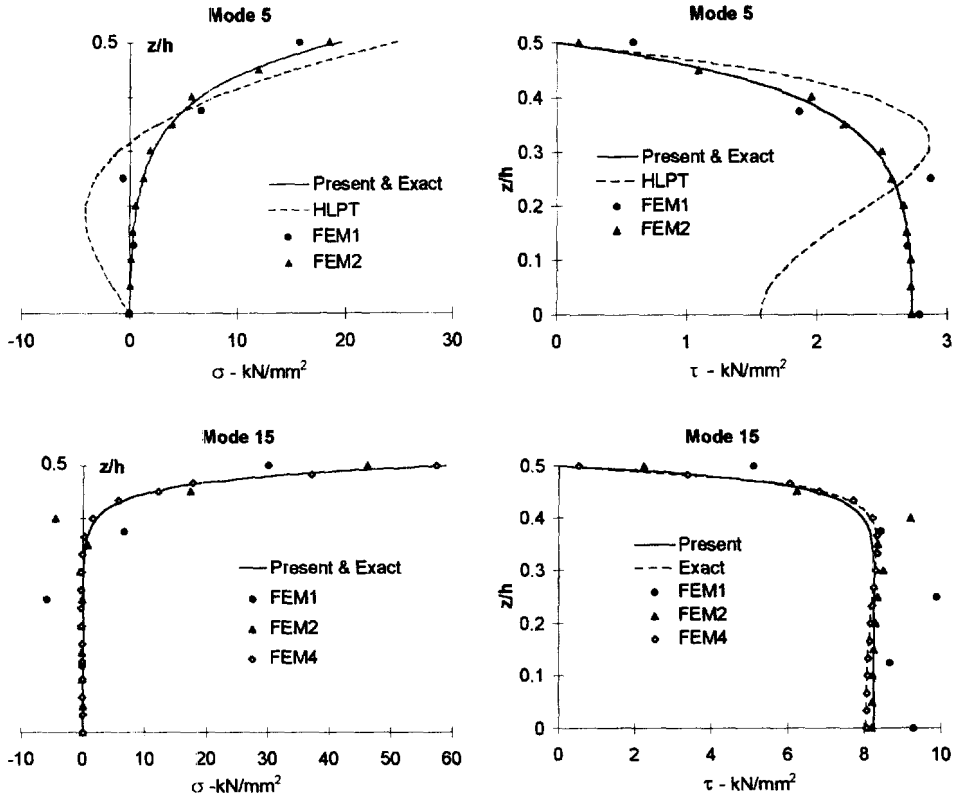

Fig. 4. Comparison of the stresses obtained by the different methods for laminate case 1.

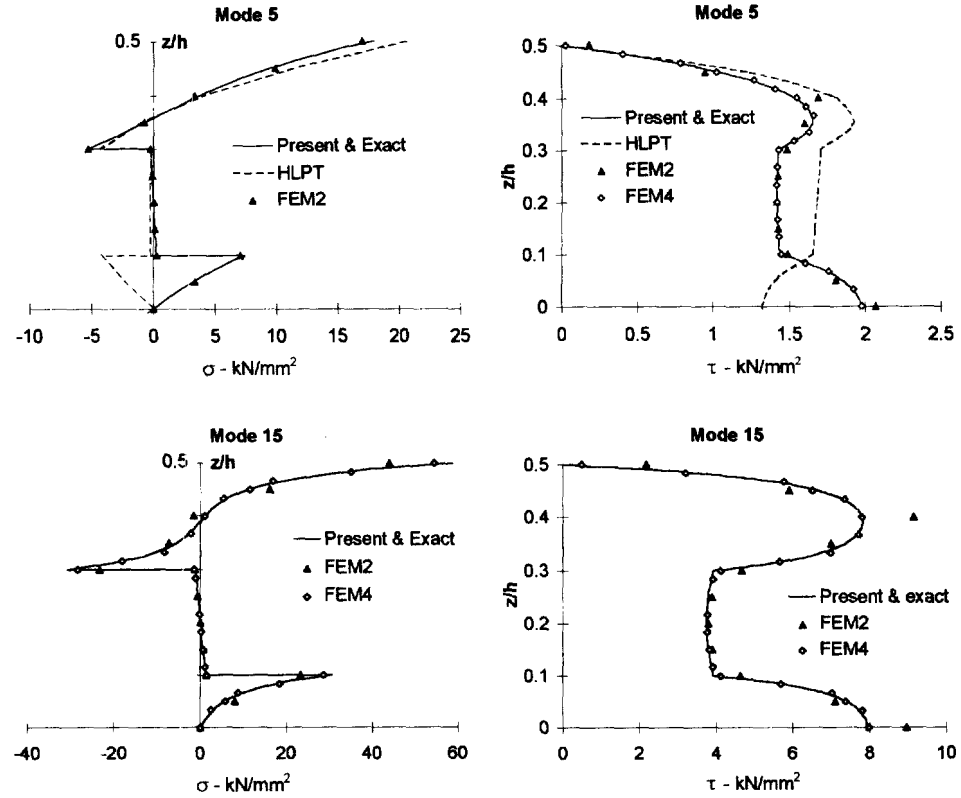

Fig. 5. Comparison of the stresses obtained by the different methods for laminate case 2.

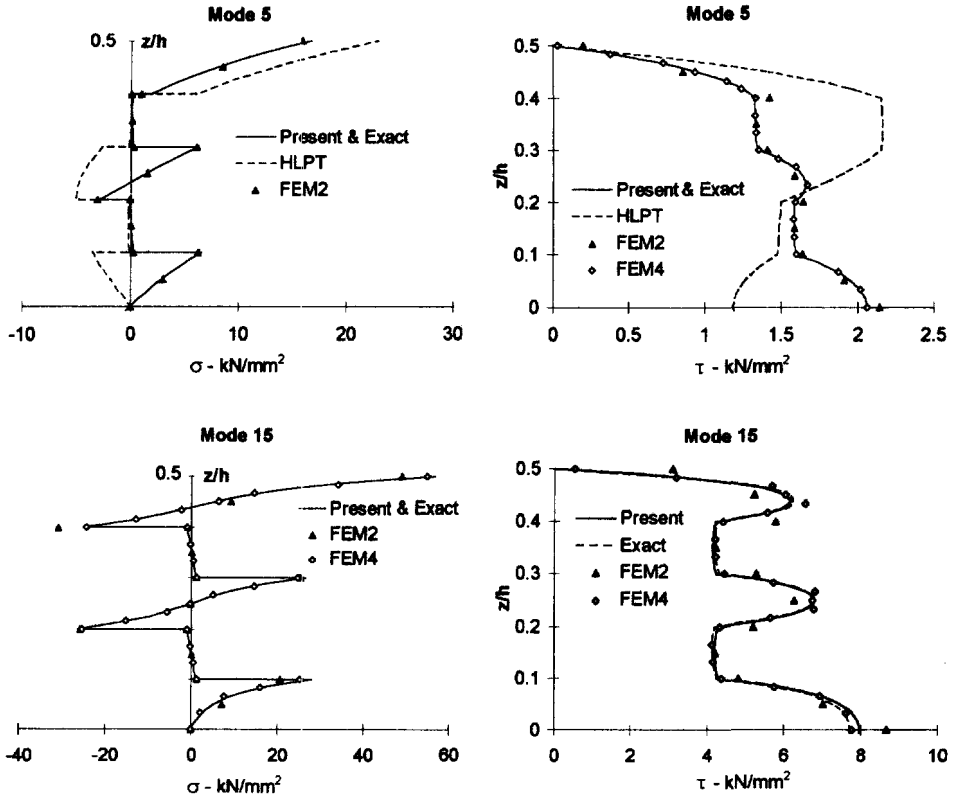

Fig. 6. Comparison of the stresses obtained by the different methods for laminate case 3.

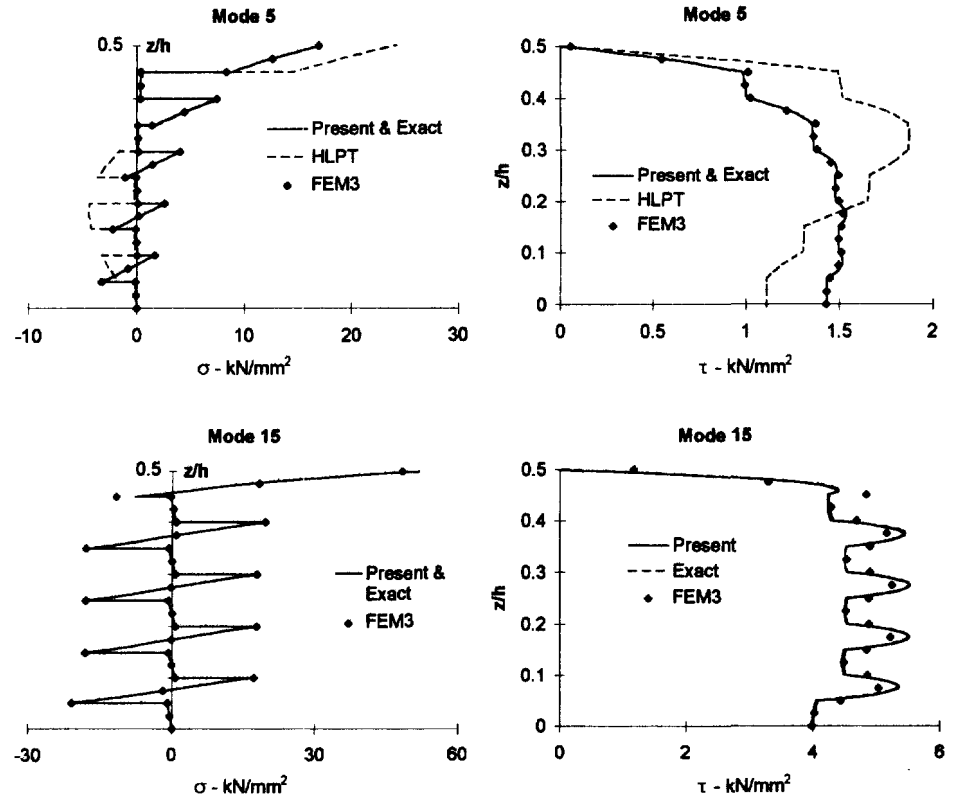

Fig. 7. Comparison of the stresses obtained by the different methods for laminate case 4.

The results of FEM for different mesh schemes are also presented in Figs 4–7. With the exception of the axial stresses at the interface of two adjacent layers, all other stresses are the nodal average stresses. At the interface of the two adjacent layers the average nodal axial stresses would lead to incorrect results and therefore, the element nodal stresses were considered. The investigation has been done for modes 5, 15 and 27, however, for the sake of brevity only the results of modes 5 and 15 are presented in these figures.

The results of the three FEM idealizations for case 1 are presented in Fig. 4. As the figure shows, the FEM model with coarse mesh cannot predict the stresses accurately. The discrepancy of the results increases as the mode number increases. The FEM idealization with scheme 1 is incapable of generating reasonable results, even for mode 5. The divergency from the exact solution increases as higher modes are considered. For mode 27 the maximum axial stress obtained by FEM using mesh scheme 1 is about one third of the exact value and the maximum shear stress is about 30% higher than the exact value. By adopting finer meshes, the results converge to the exact values. Also, as the number of mode increases, a finer mesh scheme is required. For example, although mesh scheme 2 produces reasonable results for mode 5, it generates inaccurate results for higher modes (i.e. 15 and 27). The same behavior holds for mesh scheme 4. This mesh scheme gives a good result for mode 15. However, for mode 27 the predicted maximum axial stress is about 20% less than the exact value. The results of FEM analysis for laminate cases 2 and 3 are plotted in Figs 5 and 6. The results shows the similar behavior as in laminate case 1. However, the inaccuracy of shear stresses at the interface of two adjacent layers is much higher than the other places.

The FEM analysis of laminate case 4 has been done only by using mesh scheme 3, presenting the thickness of each layer by one quadratic element. Because of having 20 layers, it was impractical to use the other mesh schemes for the laminate. The results of FEM analysis are presented in Fig. 7. The accuracy of the shear stresses and also the axial stresses in the outer most layer for modes 15 and 27 is not good. The inaccuracy of the shear stresses at the interface of two adjacent layers is much higher.

SUMMARY AND CONCLUSION

The analytical solution based on through-the-thickness inextensibility of plate, for static loading was given before (Jalali and Taheri, 1998). The solution has been extended for treating the transverse vibration of simply-supported cross-ply laminated plates in cylindrical and/or planar condition. A new procedure was also employed to increase the capability of the exact solution given by Jones (1970). Laminates with different numbers of layers (up to 20 layers) were examined. The natural frequencies of several modes as well as the corresponding stresses were obtained using the proposed method and the exact solution. Also, the problems were analyzed by the finite element method (FEM) and the higher-order laminated plate theory (HLPT) formulated by Reddy (1989). The comparison of the results obtained by the different methods concludes the following:

(1) The accuracy of the natural frequencies obtained by the proposed method depends on the number of layers in the laminate and mode number. For $mh/L < 2$ the results obtained for all the cases are practically identical to the exact values. This pattern persisted for the unidirectional laminate and the laminates consisting of several layers (say 15 and more), even for $mh/L > 2$. For the other types of laminates, discrepancy increases as mh/L increases.

(2) The effect of rotary inertia is negligible.

(3) The natural frequencies obtained by HLPT are not very accurate, and they depend on the value of mh/L. The discrepancy of the results of HLPT for all cases goes beyond 6%.

(4) The stresses obtained by the proposed method are very close to the exact values and in most cases they are practically identical. However, in general, discrepancy increases by the increase of the mh/L value.

(5) The stresses obtained by HLPT, even for small value of mh/L (say 0.1) are not very accurate. The discrepancy increases rapidly for higher modes. The results for $mh/L > 0.3$ are not acceptable.

(6) The results of FEM converge to the exact values by increasing the mesh density. However, for a specified mesh density, the accuracy of the result decreases as the mode number increases. The results of the analysis for mode 27 using 4500 quadratic plane strain elements modeling a half symmetry of the plate showed considerable frequency for stress values. In general, the shear stresses at the interface of two adjacent layers have much less accuracy than those calculated at other locations. Obtaining an accurate results for practical problems consisting of a large number of layers (more than 50) for higher modes may not be possible without access to substantial computational power and resources.

Recognizing the problem involved with HLPT and FEM in predicting the stresses under higher modes, the advantage of present method becomes clear. On the other hand, the applicability of the exact solution is limited. Even though the procedure employed in this paper remarkably increases the capability of the exact solution, the procedure uses the results obtained by the present method as an initial data. The required computation time for the exact solution is about 16 times more than the present model for only one iteration. This is due to the fact that there is only one unknown per layer for the present method, while for the exact solution each layer has four unknowns. Furthermore, for the problems solved in the present work the minimum number of iterations was about 40.

We believe that the methodology outlined in this paper in conjunction with modal analysis is an effective and efficient tool in predicting the correct response and stress distribution of composite laminated plates subjected to transversal dynamic loading. It is worthwhile mentioning that, as for most analytical solutions, the applicability of the proposed solution is limited to structures with simple geometry. Nevertheless, the solution is useful for preliminary investigations and research purposes. It can also be used as a mean for validating the results obtained by other approximate, yet practical methods. For more general problems one must resort to elasticity based FEM (as we used in this work) or FEM based on layerwise laminated theories, such as those proposed by, for example, Reddy (1989), Basar *et al.* (1993), and Robbins and Reddy (1993).

Acknowledgement—The work presented was supported by a scholarship of the Ministry of Culture and Higher Education of Islamic Republic of Iran to the first author, and NSERC operating grant no. OGP0090736, awarded to the second author. The authors are grateful to these agencies.

REFERENCES

Basar, Y., Ding, Y. and Schultz, R. (1993) Refined shear-deformation models for composite laminated with finite rotations. *International Journal of Solids and Structures* **30,** 2611–2638.

Jalali, S. J. and Taheri, F. (1998) An analytical solution for cross-ply laminates under cylindrical bending based on through-the-thickness inextensibility. Part I—static loading. *International Journal of Solids and Structures* **35,** 1559–1574.

Jones, A. T. (1970) Exact natural frequencies for cross-ply laminates. *Journal of Composite Materials* **4,** 476–491.

Kulkarni, S. V. and Pagano, N. J. (1972) Dynamic characteristics of composite laminates. *Journal of Sound and Vibration* **23,** 127–143.

NISA II, User's manual (1995) Engineering Mechanics Research Corporation, Troy, MI.

Reddy, J. N. (1989) On refined computational models of composite laminates. *International Journal for Numerical Methods in Engineering* **27,** 361–382.

Reddy, J. N. and Khdeir, A. A. (1989) Buckling and vibration of laminated composite plates using various plate theories. *AIAA Journal* **27,** 1808–1817.

Robbins, Jr, H. D. and Reddy, J. N. (1993) Modelling of thick composites using a layerwise laminate theory. *International Journal for Numerical Methods in Engineering* **36,** 655–677.